Bioorganic & Medicinal Chemistry Letters 24 (2014) 54–60

Contents lists available at ScienceDirect

Bioorganic & Medicinal Chemistry Letters

journal homepage: www.elsevier.com/locate/bmcl

# Synthesis, biological evaluation and SAR of 3-benzoates of ingenol for treatment of actinic keratosis and non-melanoma skin cancer

Gunnar Grue-Sørensen [a], Xifu Liang [a], Kristoffer Månsson [a], Per Vedsø [a], Morten Dahl Sørensen [a], Anke Soor [a], Martin Stahlhut [b], Malene Bertelsen [b], Karen Margrethe Engell [c], Thomas Högberg [a,*]

[a] Chemical Research, LEO Pharma A/S, 55 Industripaken, DK-2750 Ballerup, Denmark
[b] Biological Research, LEO Pharma A/S, 55 Industriparken, DK-2750 Ballerup, Denmark
[c] Product Reprofiling, LEO Pharma A/S, 55 Industriparken, DK-2750 Ballerup, Denmark

ARTICLE INFO

*Article history:*
Received 23 October 2013
Revised 24 November 2013
Accepted 29 November 2013
Available online 4 December 2013

*Keywords:*
Ingenol 3-benzoates
PKCδ activation
Oxidative burst
Cytokine release
Cell death induction
Molecular modeling

ABSTRACT

Ingenol 3-benzoates were investigated with respect to chemical stability, pro-inflammatory effects, cell death induction and PKCδ activation. A correlation between structure, chemical stability and biological activity was found and compared to ingenol mebutate (ingenol 3-angelate) used for field treatment of actinic keratosis. We also provided further support for involvement of PKCδ for induction of oxidative burst and cytokine release. Molecular modeling and dynamics calculations corroborated the essential interactions between key compounds and C1 domain of PKCδ.



Ingenol mebutate (PEP005, ingenol 3-angelate, **1**), the active ingredient in Picato®, a new drug for field treatment of actinic (solar) keratosis (AK),[1] is isolated from *Euphorbia peplus* plants (Fig. 1).[1,2] Ingenol mebutate and other ingenol 3-acylates are potent activators of protein kinase C (PKC) responsible for a number of essential cellular signal transduction responses.[3,4] The clinical efficacy of ingenol mebutate against actinic keratosis is believed to be linked to a dual mechanism of action, that is (i) induction of keratinocyte cell death and (ii) induction of a lesion-directed immune response, at least partially mediated by PKC.[5] This profile accounts for high clearance rates after only 2–3 days of topical field treatment of AK lesions with a predictable onset and short duration of local skin responses.[1] In addition, patients treated with ingenol mebutate gel also experience sustained clearance of AK lesions one year later.[6]

For decades natural products have been a great source of inspiration for the pharmaceutical industry and minor changes of complex structures isolated from nature have led to a number of potent drugs.[7] In our search for novel analogues of ingenol mebutate with improved properties, such as chemical stability, potency and efficacy towards non-melanoma skin neoplasia such as actinic keratosis, basal cell carcinoma (BCC), squamous cell carcinoma (SCC) and Bowen's disease,[8]

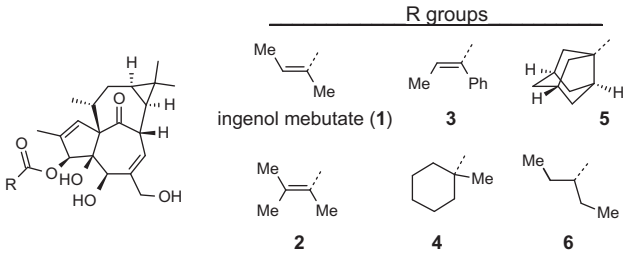


**Figure 1.** 3-Acyl ingenol derivatives **2**–**6** with favorable properties comparable to ingenol mebutate (**1**).[9]

we have previously investigated the consequences of minor structural changes of the ingenol scaffold of **1** as well as the replacement of the 3-angelate group with other aliphatic acylates.[9] The rigid ingenol scaffold convey several structural features, including the 5- and 20-hydroxyl groups, essential for biological activity. Only a small number of compounds **2**–**6** with comparable or slightly improved overall profile over **1** were identified (Fig. 1). As a continuation of this work we now report on the preparation and the chemical and biological characterization of novel ingenol 3-benzoates.[10] We had also earlier provided support for the involvement of PKC activation in the pro-inflammatory effects such as release of cytokines and reactive oxygen species (ROS).[9] In this work we have extended this aspect further by showing

* Corresponding author. Tel.: +45 44 94 58 88.
*E-mail address:* thomas.hogberg@leo-pharma.com (T. Högberg).

0960-894X/$ - see front matter © 2013 Elsevier Ltd. All rights reserved.
http://dx.doi.org/10.1016/j.bmcl.2013.11.073

correlations between these parameters as well as modeling and dynamic studies of key molecules interacting with PKCδ.

The preparation of new 3-benzoyl derivatives of ingenol follows previously described methods shown in Scheme 1.[9,11,12] Ingenol 5,20-acetonide (**7**) was isolated after crystallization, and standard procedures, such as Steglich coupling conditions or using acyl chlorides, were applied in the preparation of **I**.[9] As will become clear in the following discussion we were introducing increasingly sterically hindered acids which also called for use of microwave (μw) assisted reactions in pressure vials at short reaction times. The final acid catalyzed deprotection step to produce the benzoate esters **II** was based on our modified procedure.[9,12] For the preparation of anthranilic acid esters **VII**, **IX** and **X** we first converted the anthranilic acids **III** into the isatoic anhydrides **IV**, which were *N*-methylated to give **V**. The isatoic anhydrides **IV** and **V** were reacted with ingenol 5,20-acetonide **7** to give **VIII** and **VI**, respectively (Scheme 2). Subsequent N-acylation with acyl chlorides or N-alkylation via reductive aminations followed by deprotection provided the modified anthralinate esters **VII**, **IX** and **X**. Likewise, the preparation of salicylic acid ester **32** required *O*-protection with an allyl group and conversion to 2-*O*-allyl-6-methyl-salicylic chloride which was reacted with ingenol 5,20-acetonide **7** as shown in Scheme 3. Palladium catalyzed removal of the allyl group followed by the normal acidic acetonide deprotection provided the salicylate **32**.

The biological activity profile was evaluated as previously described.[9,13] The induction of necrotic cell death was determined in HeLa cells. The activation of the immune response was measured as induction of oxidative burst (i.e., generation of ROS) in polymorphonuclear leukocytes and the release of the cytokines IL8 and TNFα in human primary keratinocytes. Furthermore, the activation of PKCδ was determined for several compounds to explore the correlation to ROS and cytokine release potency.[14]

Chemical stability is essential to ensure sufficient shelf-life of drugs. Ingenol mebutate (**1**) is most stable at pH 2.0–4.5 and, as previously described, the 3-angelate undergoes acyl migration in aqueous solution to form an equilibrium mixture between the 3-, 5- and 20-mono-angelates in ratios of about 1:1:18 with no immediate hydrolysis.[9] The 5-hydroxyl group is critical for this pH-dependent degradation mechanism,[15] but this group is also a prerequisite for biological activity.[9] Bulkiness (steric hindrance) of the 3*O*-acyl groups has been shown to be an important factor

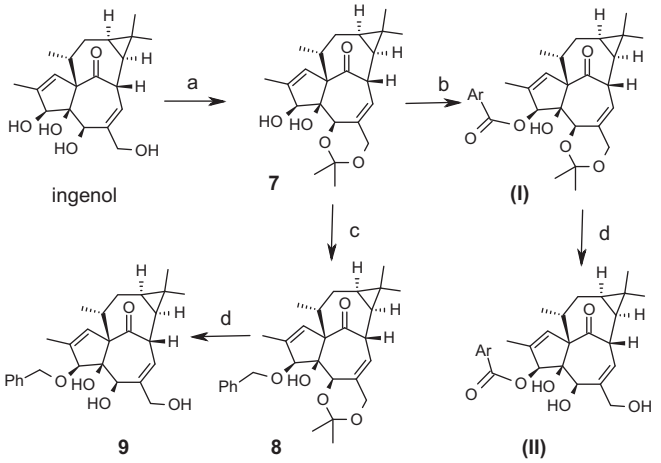


**Scheme 1.** General synthetic route from ingenol to ingenol 3-benzoates **II** and benzyl ether **9**. Reagents and conditions: (a) acetone, PTSA (cat), rt, 0.5 h, 73%; (b) $ArCO_2H$, DCC, DMAP, MeCN, rt → 140 °C (μw); or ArCOCl, DMAP, DIPEA, MeCN, rt → 140 °C (μw); (c) benzyl bromide (5 equiv), $Cs_2CO_3$ (6 equiv), MeCN, 150 °C (μw), 5 min. 62%; (d) aq HCl/THF; or aq HCl/MeOH, rt.

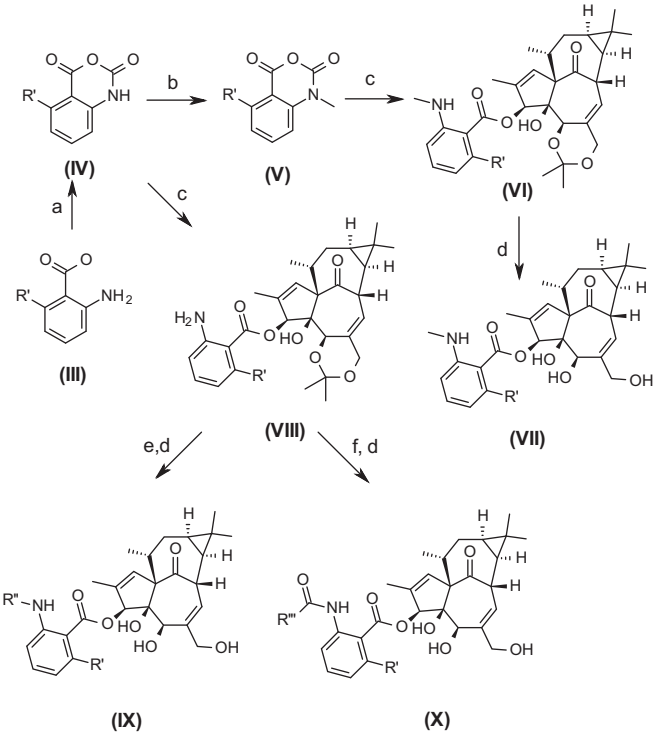


**Scheme 2.** General synthetic route from ingenol 5,20-acetonide to ingenol 3-(2-amino)benzoates **VII**, **IX** and **X**. Reagents and conditions: (a) triphosgen (1.1 equiv), THF/DCM, rt; (b) $(MeO)_2SO_2$, $K_2CO_3$, DMF, rt; (c) ingenol 5,20-acetonide **7**, DMAP, MeCN, 160 °C (μw); (d) aq HCl/THF; or aq HCl/MeOH, rt; (e) aldehyde, $NaBH(OAc)_3$, AcOH, DCM, rt; (f) acyl chloride, $K_2CO_3$, MeCN, rt.

for stability.[9] In order to quickly rank the stability of new ingenol 3-benzoates we determined the recovery at pH 7.4 after 16 h at room temperature. Under these conditions 60% ingenol mebutate was recovered. Acyl groups where the corresponding acids are weaker than angelic acid ($pK_a$ 4.3)[16] are also thought to be less prone to acyl migration, but our previous study did not indicate this factor to be of major significance.[9] For example the less acidic isomeric tiglic acid ($pK_a$ 5.0) ester was less stable (45% recovered) than the angelate ester and the less acidic cyclohexane carboxylic acid ($pK_a$ 4.9) ester was found to be equally stable as the benzoic acid ($pK_a$ 4.2) ester (30–35%, recovered).[9,16] Hence, we focused mainly on steric hindrance rather than thermodynamic acidity factors to influence the acyl migration and gain stability.

Ingenol 3-benzoate (**10**)[11] was less stable (30% recovery at our standard conditions) than ingenol 3-angelate (**1**) (Table 1). It can be noted that $pK_a$ of the corresponding acids, benzoic and angelic acid, are almost identical (4.2 and 4.3, respectively).[16] The benzoate had slightly higher oxidative burst potency, whereas the cytokine release potency was lower. This lower potency may be caused by the disappearance of the active 3-ester via acyl migration during the assay period as seen with other unstable 3-acylates.[9] The 3-benzoate **10** has previously been subject to molecular modeling studies with the crystal structure of the zinc finger domain C1 of PKCδ determined for a phorbol ester complex.[17] This domain is involved in the PKC activation induced by diacylglycerol (DAG) to release the blocking pseudosubstrate from the catalytic site, an action shared with phorbol esters.[18] Several essential hydrogen bond interactions such as with the 5- and 20-hydroxyl groups, which we have shown to play critical roles for the activity of **1**,[9] could be accounted for. Furthermore, the ester carbonyl oxygen was indicated to be engaged as a hydrogen bonding acceptor to the amide NH in Gly23 in the back-bone of the C1 domain of PKCδ.[17] To support the binding hypothesis we have prepared the

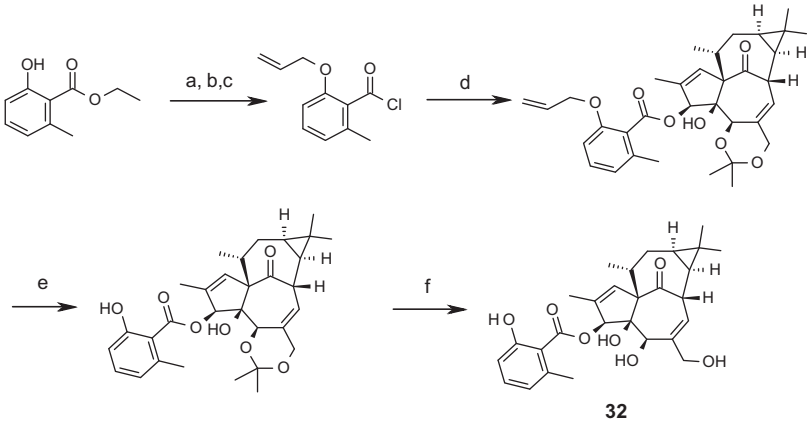


**Scheme 3.** Synthesis of salicylate **32**. Reagents and conditions: (a) allyl bromide (3 equiv), $K_2CO_3$, acetone, 90 °C (pressure tube), 3 days; (b) NaOH (2.3 equiv), MeOH/$H_2O$ (3:1), 100 °C (pressure tube), 5 h, 80 °C, 14 h; (c) $SOCl_2$, reflux, 1 h; (d) acyl chloride to ingenol 5,20-acetonide **7** (2:1), DMAP, DIPEA (2 equiv), MeCN, 100 °C (pressure tube), 1 h; (e) $Pd(Ph_3P)_4$ (0.034 equiv), $Et_2NH$, dioxane, rt, 1 h; (f) aq HCl/MeOH, rt.

benzyl ether **9** by reacting the 5,20-acetonide **7** with benzyl bromide and cesium carbonate as base catalyst to provide **8** (Scheme 1). The usual deprotection protocol produced the benzyl ether **9** in an overall yield of 40% from **7**. As expected, it showed complete chemical stability during the screening conditions and it displayed very low activity in the oxidative burst and IL8 release assays (Table 1). In accordance with these observations no activation of PKCδ was observed even at a concentration of 10 μM of **9** in contrast to the benzoate ester **10** having an $EC_{50}$ of 6.1 nM (Table 1), which supports the reported binding predictions and the importance of the ester carbonyl for activity.

To further investigate the binding of the 3-benzoate **10** to PKCδ we performed 2 ns molecular dynamics (MD) calculations of both the 3-benzoate and the 3-benzyl ether.[19,21] The MD starting conformation of 3-benzoate was obtained by docking the ligand into the crystal structure of the C1 domain of PKCδ (1PTR)[20,21] and it is in excellent agreement with the binding model proposed by Pak et al.[17] Thus, hydrogen bonds were observed between the hydroxyl groups of the ligand and Thr12, Leu21, and Gly23 in PKCδ and of particular interest between the ester carbonyl in **10** and the Gly23 NH. Furthermore, our docking model suggests a hydrophobic interaction between the side chain of Leu24 and the aromatic ring of the benzoate group (Fig. 2).

Our docking model did not indicate an interaction between the benzoate group and the side chain of Trp22 (Fig. 2a). However, an analysis of the MD trajectories strongly suggests that a rotation of the Trp22 side chain allows the aromatic ring of the benzoate group to form a stable hydrophobic sandwich with the side chains of Trp22 and Leu24 (Fig. 2b). It is also noteworthy, that the carbonyl and the phenyl ring of the benzoate is in a coplanar orientation in this hydrophobic sandwich enabling favorable π–π stacking with the indole ring of Trp22 (Fig. 2c).

Similarly, we performed a MD calculation for the benzyl ether **9**, using the benzoate **10** starting conformation but with the carbonyl reduced to a methylene.[19] Also in the case of the benzyl ether **9**, Trp22 rotates to form a hydrophobic sandwich, but the π–π stacking is not as stable as observed for the benzoate as the spread in torsion angles of the phenyl ring is in the range of ~70° compared to a more narrow span of ~40° for the ester **10** (Fig. 3). The major difference between the compounds is the lack of a hydrogen bond to Gly23 NH supporting the importance of the ester carbonyl for activity. Thus, we concentrated on the benzoate esters even if stability needed to be substantially improved. It can be noted that the benzyl ether **9** showed a reasonable necrotic effect, which indicates different mode of actions for immunostimulatory and necrotic effects.

A series of mono-substituted benzoates (Table 1) showed a clear trend that more bulkiness in the *ortho*-position favored stability. 3-Ingenol esters of *ortho*-mono-substituted benzoic acids were more stable than the unsubstituted benzoate **10** with recoveries in our standard test up to 80%. The lipophilic ingenol 3-*o*-hexadecanylamino-benzoate **23** had a relatively high recovery of 90%, but this measurement could not be carried out under our usual conditions due to the very poor solubility of the substance in aqueous buffer. We assume that highly lipophilic ingenol 3-acylates will be more stable towards acyl migration because the lipophilic acyl group will shield the ester group from the polar catalytic action of water and its dissociation products ($H^+$ and $OH^-$) (cf. Ref. 15). As stated above, the influence of acidity of the corresponding acid is subordinate to steric hindrance as the *ortho*-methoxy benzoic acid (p$K_a$ 4.1) ester **14** is considerably more stable than benzoic acid (p$K_a$ 4.2) ester **10** even if the *ortho* bromo benzoic acid (p$K_a$ 2.9) ester **11** has intermediate stability (Table 1). Hence, kinetic data are likely to reflect the migration ability better.

We explored a diverse set of *ortho*-substituted benzoates **11**–**23** containing 'neutral' (Me, *i*-Pr, Ph), electron-withdrawing (Br) and electron-donating groups of highly variable size (MeO, *i*-PrO, and $H_2N$, MeHN versus PhO, PhNH, BnHN, $C_{12}H_{25}HN$ and $C_{16}H_{33}HN$). The anilinic compounds are also capable of forming internal hydrogen bonds with the ester carbonyl group which will influence the orientation of the aniline substituent and favoring a coplanar conformation and affecting the ability of the carbonyl (benzoate group) to engage in the postulated interaction in PKCδ. Notably, the potency of oxidative burst activation did not change significantly within the series of the *ortho*-mono-substituted derivatives compared to the potency of ingenol 3-benzoate **10** (Table 1). Only ingenol 3-*o*-methoxy-benzoate (**14**) appeared to be somewhat less potent in the cytokine release assay, contrasting to the slightly more bulky *o*-isopropoxy derivative **15** with a 10-fold higher potency. The methoxy derivative also displayed the lowest PKCδ activation potency (25.7 nM) of the investigated *ortho*-mono-substituted benzoates (Table 1). Otherwise, most of the *o*-mono-substituted benzoates tested were superior, i.e., **11**, **13**, **15**–**21**, to ingenol mebutate. In terms of chemical stability, several compounds had somewhat improved stability over the angelate 1, with the phenyl **16** and phenoxy **17** being the most stable with ~80% recovered (Table 1). The most lipophilic aniline **23** had good stability, but was an outlier with poor potency in the oxidative burst and cytokine release assays. Poor solubility of this compound made determination of necrotic potential impossible.

We then added extra steric hindrance (cf. Ref. 22) to the benzoates with the introduction of two flanking ortho-substituents.

**Table 1**
Chemical stability and biological activity of ingenol 3-benzoates compared to ingenol mebutate (**1**) and benzyl ether **9**

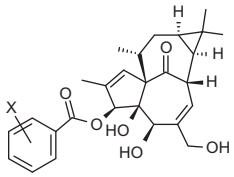


| No. | X | Stability[a] | Oxidative burst[b] | | TNFα release[c] | | IL8 release[c] | | Necrosis[d] | PKCδ[e] |
|---|---|---|---|---|---|---|---|---|---|---|
| | | % Recovered | $EC_{50}$ (nM) | $E_{max}$ (%) | $EC_{50}$ (nM) | $E_{max}$ (%) | $EC_{50}$ (nM) | $E_{max}$ (%) | $LC_{50}$ (μM) | $EC_{50}$ (nM) |
| Angelate **1** | NA | 60 | 8.7 | 113 | 11.2 | 98 | 10.3 | 95 | 230 | 4.1 |
| Benzyl **9** | NA | >95 | 4540 | — | Nd | — | 4520 | 58 | 378 | >10,000 |
| **10** | H | 30 | 6.0 | 110 | 88 | 60 | 182 | 54 | Nd | 6.1 |
| **11** | 2-Br | 44 | 4.3 | 99 | 8.2 | 96 | 2.3 | 93 | 141 | 3.8 |
| **12** | 2-Me | 73 | 5.7 | 107 | 13 | 64 | 15 | 58 | 115 | Nd |
| **13** | 2-*i*Pr | 70 | 11 | 120 | 5.7 | 96 | 4.4 | 86 | 110 | Nd |
| **14** | 2-MeO | 70 | 6.8 | 107 | 38 | 100 | 42 | 100 | 220 | 25.7 |
| **15** | 2-iPrO | 65 | 8.7 | 113 | 4.0 | 101 | 2.7 | 105 | 192 | Nd |
| **16** | 2-Ph | 77 | 16 | 105 | 1.6 | 91 | 1.5 | 87 | 77 | 3.3 |
| **17** | 2-PhO | 80 | 9.4 | 98 | 1.4 | 86 | 1.1 | 87 | 83 | 13.1 |
| **18** | 2-PhNH | 58 | 11 | 129 | 5.0 | 120 | 3.7 | 103 | 307 | 4.2 |
| **19** | 2-$NH_2$ | 58 | 15 | 116 | 5.5 | 112 | 3.4 | 101 | 199 | Nd |
| **20** | 2-MeNH | 68 | 6.7 | 113 | 1.0 | 134 | 0.79 | 99 | 95 | 2.5 |
| **21** | 2-BnNH | 65 | 8.6 | 127 | 1.5 | 128 | 1.2 | 115 | 168 | Nd |
| **22** | 2-$C_{12}H_{25}NH$ | Nd[f] | 25 | 78 | 14 | 150 | 16 | 111 | 400 | Nd |
| **23** | 2-$C_{16}H_{33}NH$ | 90 | 1340 | 94 | 200 | 120 | 61 | 125 | Nd | Nd |
| **24** | 2,6-$Me_2$ | >95 | 13 | 123 | 83 | 61 | 62 | 66 | 97 | 10.8 |
| **25** | 2,6-$MeO_2$ | >95 | 84 | 116 | 57 | 113 | 44 | 107 | 400 | 156 |
| **26** | 2,6-$Cl_2$ | >95 | 21 | 123 | 278[g] | 42 | 113[g] | 45 | 59 | 19.8 |
| **27** | 2-Me, 6-Cl | >95 | 6.6 | 130 | 54 | 52 | 51 | 52 | 126 | Nd |
| **28** | 2-Me, 6-$NH_2$ | >95 | 8.6 | 117 | 12 | 108 | 8.2 | 118 | 146 | 8.0 |
| **29** | 2-MeO, 6-$NH_2$. | >95 | 25 | 109 | 108 | 83 | 41 | 111 | Nd | Nd |
| **30** | 2-Cl, 6-$NH_2$ | 93 | 7.1 | 161 | 28 | 108 | 20 | 104 | 185 | Nd |
| **31** | 2-F, 6-$NH_2$ | 66 | 12 | 133 | 10 | 104 | 8.6 | 104 | 201 | Nd |
| **32** | 2-Me, 6-OH | >95 | 9.4 | 125 | 98 | 156 | 71 | 105 | 199 | 13.4 |
| **33** | 2-Me, 6-MeNH | >95 | 46 | 136 | 16 | 143 | 12 | 127 | 105 | Nd |
| **34** | 2-Cl, 6-MeNH | >95 | 21 | 124 | 21 | 97 | 18 | 105 | 145 | Nd |
| **35** | 2-F, 6-MeNH | 74 | 9.3 | 123 | 4.1 | 174 | 3.0 | 145 | 152 | Nd |
| **36** | 2-Me, 6-BnNH | >95 | 42 | 103 | 7.6 | 126 | 3.8 | 122 | 187 | Nd |
| **37** | 2-MeO, 6-BnNH | >95 | 23 | 112 | 19 | 120 | 6.6 | 117 | 400 | Nd |
| **38** | 2-Me, 6-AcNH | 82 | 538 | 113 | 632 | 92 | 534 | 92 | Nd | 988 |
| **39** | 1-Naphthoyl | 42 | 11 | 116 | 3.3 | 119 | 2.3 | 97 | 87 | 3.7 |

[a] The chemical stability over 16 h was evaluated in an aqueous buffer with less than 30% organic solvent at pH 7.4. Reported as % recovered material.[25]
[b] PMN respiratory burst after 40 min incubation of test compound was quantified by measuring fluorescence expressed in relative light units.[26] $EC_{50}$ denotes the test compound concentration producing 50% of the maximum effect given by **1**. $E_{max}$ indicates the maximal response in relation to **1**.
[c] Cytokine secretions were measured in human adult log-phase primary epidermal keratinocytes after incubation of test compound for 6 h at 37 °C.[27] The $EC_{50}$ and $E_{max}$ calculations according oxidative burst protocol.
[d] HeLa cells were treated with test compounds for 30 min at 37 °C and then measured remaining the metabolic activity. $LC_{50}$ denotes concentration giving 50% loss of metabolic activity.[28]
[e] Activation potency of PKCδ was measured by the use of an in vitro phosphorylation assay using a PKC-peptide substrate (40 min, room temperature).[29]
[f] Nd: not determined.
[g] Concentrations yielding maximum responses are given.

*ortho*-Methyl, *o*-methoxy, *o*-chloro and *o*-amino substituents provided enough steric bulkiness, provided both *ortho*-positions were substituted as in compounds **24**–**30**, to give stable ingenol 3-benzoates with 'complete' stability, that is >95% recovery under our assay conditions (Table 1). The importance of substituting both *ortho*-positions in order to gain stability is clearly shown when comparing the two isomers ingenol 3-(2-methylamino-benzoate)[23] (**20**) and 3-(2-amino-6-methyl-benzoate) (**28**). Introduction of *o*-hydroxy as another group than *o*-amino capable of internal hydrogen bonding provides a compound that is comparable on oxidative burst but 10-fold less active on cytokine release (**32** vs **28**).

As expected, introduction of an *o*-fluor did not contribute significantly to the stability, and cytokine release potency dropped slightly compared to the hydrogen analogues (**31** vs **19** and **35** vs **20**). Notably, an even larger drop in cytokine release potency is seen for the corresponding *o*-chloro derivatives (**30** and **34**). The 2-naphtoate ester (**39**) did not provide enough steric hindrance to give a stable ester (42% recovery), albeit cytokine release potency was superior to that of ingenol mebutate and the unsubstituted benzoate **10**.

The *o*,*o*-disubstituted benzoates were, in general, more stable than the *o*-mono-substituted benzoates, but this increase in stability was apparently associated with a decrease in oxidative burst and cytokine release potency. The most promising disubstituted benzoates with respect to cytokine release potency contained an *o*-amino group, either unsubstituted (**28**, **31**) or *N*-mono-substituted (**33**–**37**), of which the 2-fluoro-6-methylamino-benzoate **35** and 2-methyl-6-benzylamino-benzoate **37** were slightly superior to ingenol mebutate in the cytokine release. As observed for the mono-substituted benzoates an *o*-methoxy substituent had a negative effect on potency compared to *o*-methyl (**29** vs **28** and **37** vs **36**), albeit the difference is smaller for the larger benzylamine compounds than for the primary anilines.

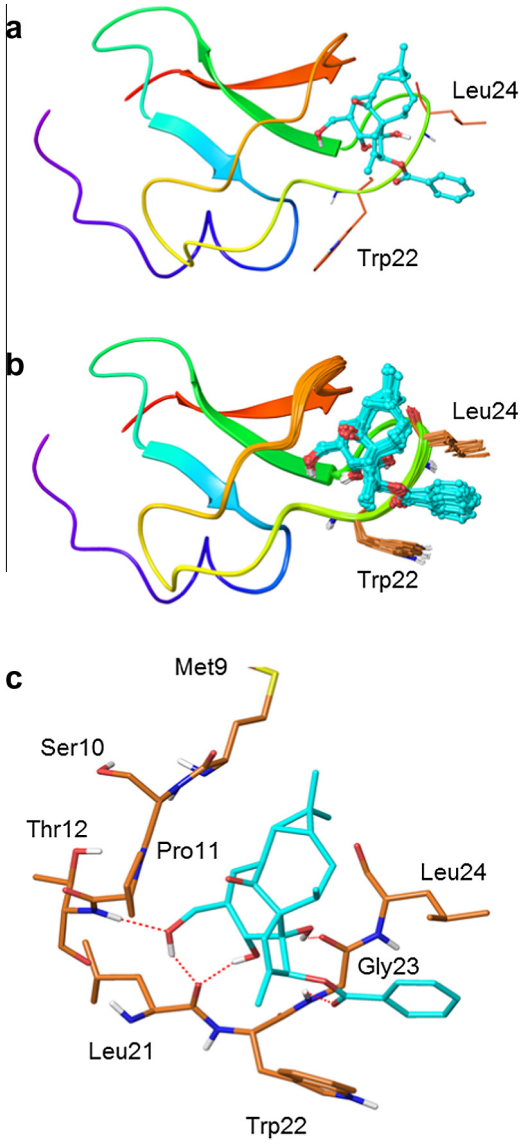


**Figure 2.** (a) Ingenol 3-benzoate **10** (cyan) docked into the crystal structure of the zinc finger C1 domain of PKCδ (1PTR). Residues Trp22 and Leu24 are shown in orange. (b) Snapshot taken every 100 ps from a 2 ns MD calculation of **10** in PKCδ. (c) Binding interactions between the benzoate **10** and PKCδ with the essential residues.[19–21] (The figure was made in Maestro, Schrödinger, LLC, New York, NY, 2013.)

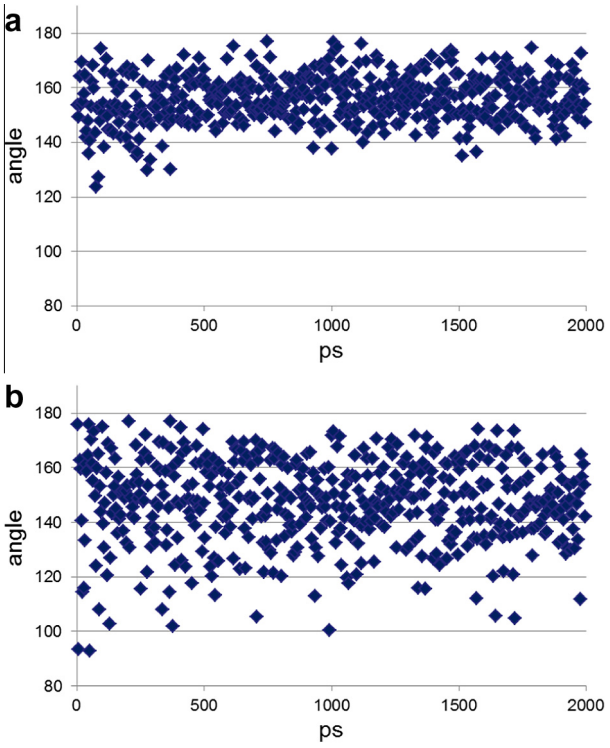


**Figure 3.** Analysis of the co-planarity of the ligand phenyl ring and the indole ring of Trp22. (a) Ring plane angles from the MD calculation of ingenol-3-benzoate **10** bound to PKCδ. (b) Ring plane angles from the MD calculation of ingenol-3-benzyl ether **9** bound to the C1 domain of PKCδ.[19,21]

Ingenol 3-(2-methyl-6-methylamino)-benzoate (**33**) is moderately active in the cytokine release assays, but insertion of a carbonyl group in the methylamino moiety to give an acetamido group (**38**) had a strong negative effect on potency. The acetamido compound **38** also showed a very modest PKCδ activation with an $EC_{50}$ of ~1 μM (Table 1) supporting the link between PKC activation and ROS and cytokine release.

By increasing the stability of ingenol 3-acylates by increasing the steric hindrance of the acid, there is a priori a risk that the benzoate carbonyl group and aromatic ring will be forced out of the co-planar orientation which seems optimal for interaction with the target protein as illustrated with PKCδ (Fig. 2). In fact, as shown above, there is a tendency for the bulky and stable 2,6-disubstituted benzoates towards lower potency, which indicates that the fixation of the carbonyl group away from a favorable position for acyl migration at the same time is sub-optimal for PKC activation. In accordance with the MD calculations, our SAR data indicate a preferred coplanar orientation of the benzoate ring and the carbonyl for optimal effects on ROS and cytokine release. This led us to speculate that the favorable combination of stability and biological effects seen with some 6-substituted 2-anilinic derivatives, such as **28**, is driven by a closer coplanar arrangement via the intramolecular hydrogen-bond tendency. Quantum mechanical (QM) optimization[24] of different 2,6-disubstituted benzoate systems confirmed that the 2-anilinic substituent does indeed favor a co-planar orientation whereas for example 2,6-dimethyl substitutions result in a twisted orientation as shown in Figure 4.

To further explore this relationship, the PKCδ activity was measured for a number of compounds (Table 1) and the correlations between oxidative burst and cytokine release on the one side and PKCδ activation on the other side were investigated (Fig. 5). Taken the considerations into account that the data set is somewhat skewed containing mostly potent compounds the following conclusions can be reached. As expected a strong correlation ($r^2$ = 0.999) was found between PKCδ activation and induction of oxidative burst (Fig. 5a).[14] The potency for release of the two cytokines IL8 and TNFα were also very closely correlated (Fig. 5b), but only a moderate correlation was reached between PKCδ and IL8/TNFα release as the significance was driven by one or two compounds (cf. IL8 data in Fig. 5c). Accordingly, a less impressive correlation was found between IL8 and oxidative burst as the high correlation coefficient ($r^2$ = 0.96) is once again biased by two compounds as shown in Figure 5d. These differences may be related to different cellular PKC profile and the fact that different ingenol derivatives could display differences in their PKC selectivity. Besides, the stability of the compounds could influence the cytokine release potency as the assay is run for 6 h which might give rise to a lower cytokine release potency than in the in vitro kinase assay or in respiratory burst which are measured after 40 min, as highlighted with benzoate **10** indicated with an arrow in Figure 5c

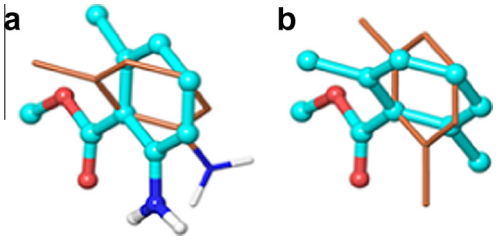


**Figure 4.** (a) Quantum mechanical (QM) optimization of a twisted conformation of 2-Me, 6-$NH_2$ benzoate (**28**) results in a co-planar orientation (cyan). (b) QM optimization of a planar conformation of 2,6-$Me_2$ benzoate (**24**) results in a twisted orientation (cyan). The starting conformations are shown in orange.[21,24] (The figure was made in Maestro, Schrödinger, LLC, New York, NY, 2013).

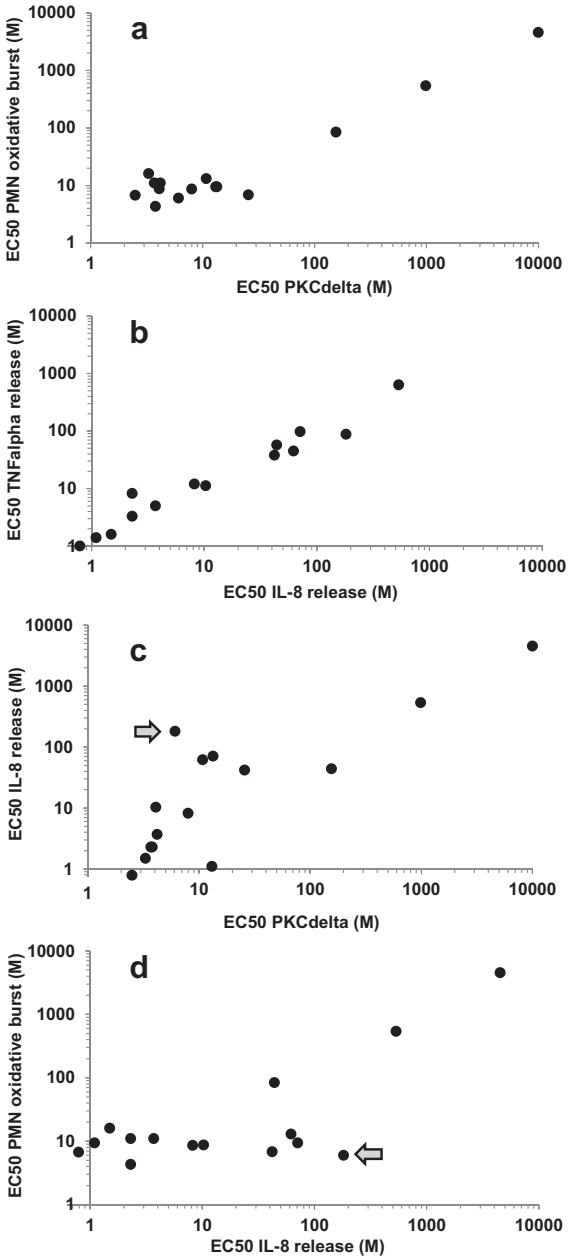


**Figure 5.** (a) Plot of $EC_{50}$'s for PKCδ activation versus oxidative burst; (b) Plot of $EC_{50}$'s for release of IL8 versus release of TNFα; (c) Plot of $EC_{50}$'s for PKCδ activation versus IL8 release; (d) Plot of $EC_{50}$'s for IL8 release versus oxidative burst. Arrows indicate the unstable ingenol 3-benzoate (**10**).

and d, respectively. Even if we have mostly determined PKCδ activation on relatively potent compounds, the compounds **25** and **38** support that poor oxidative burst and cytokine release potency relates to poor PKCδ activation.

For most compounds in Table 1, induction of cell death takes place at concentrations of about 60–200 μM that are more than four orders of magnitude higher than the concentrations of about 1–20 nM needed for PKCδ activation (Table 1). All benzoate compounds in Table 1 (with the exception of the methoxy-substituted benzoates **25** and **37** and the lipophilic compounds **22** and **18**) appear to have a higher necrotic potential than ingenol mebutate, and this is probably an indication of a mechanism for the necrosis that is not primarily linked to PKCδ activation. The mechanism for cell death induction is currently under investigation.[5d]

We conclude that it is possible to prepare chemically stable ingenol 3-acylates, albeit in general, with lower potency in ROS and cytokine release. However, the potent monosubstituted *o*-phenyl and *o*-phenoxy derivatives **16** and **17**, respectively, also have significantly improved chemical stability and 10-fold higher potency on cytokine release compared to ingenol mebutate (**1**). Furthermore, we found a narrow span of 2,6-substituted anilinic derivatives, for example **28**, **30**, and **34**, with an attractive profile of very good stability and reasonable potency in ROS and cytokine release as well as with a good necrotic potential. Our investigation also provided strong support for a causative link between PKC activation and ROS and cytokine release in accordance with our previous SAR studies.[9] These findings were corroborated by modeling studies indicating a crucial role of the carbonyl oxygen as well as a preferable relatively coplanar orientation of the carbonyl and the phenyl ring of the benzoates when interacting with PKC.

Pharmacological in vivo experiments are ongoing to test the utility of these molecules in the treatment of actinic keratosis and possibly non-melanoma carcinomas (e.g., BCC, SCC and Bowen's disease)[8] as they display pronounced effects on inducing necrotic cell death combined with the desirable immunostimulatory properties and improved chemical stability.

## Acknowledgments

We acknowledge Thomas Vifian, Karin Hvidtfeldt Hansen, Svitlana Tkach, Christa Marvig, Carsten Ryttersgaard, Nina Ravn Borch, Ninette Winther Hansen, Nannette Svendsen for skillful assistance.

## References and notes

1. (a) Lebwohl, M.; Swanson, N.; Anderson, L. L.; Melgaard, A.; Xu, Z.; Berman, B. N. *Engl. J. Med.* **2012**, *366*, 1010; (b) Lebwohl, M.; Sohn, A. *Expert Rev. Dermatol.* **2012**, *7*, 121; (c) Berman, B. *Clin. Cosmet. Invest. Dermatol.* **2012**, *5*, 111; (d) Ali, F. R.; Wlodek, C.; Lear, J. T. *Dermatol. Ther.* **2012**, *2*, 8; (e) Martin, G.; Swanson, N. *J. Am. Acad. Dermatol.* **2013**, *68*, S39; (f) Keating, G. M. *Drugs* **2012**, *72*, 2397.
2. (a) Vasas, A.; Rédei, D.; Csupor, D.; Molnár, J.; Hohmann, J. *Eur. J. Org. Chem.* **2012**, 5115; (b) Hohmann, J.; Evanics, F.; Berta, L.; Bartók, T. *Planta Med.* **2000**, *66*, 291.
3. (a) Winkler, J. D.; Hong, B.-C.; Bahador, A.; Kazanietz, M. G.; Blumberg, P. M. *Bioorg. Med. Chem. Lett.* **1993**, *3*, 577; (b) Winkler, J. D.; Kim, S.; Harrison, S.; Lewin, N. E.; Blumberg, P. M. *J. Am. Chem. Soc.* **1999**, *121*, 296.
4. (a) Bosco, R.; Melloni, E.; Celeghini, C.; Rimondi, E.; Vaccarezza, M.; Zauli, G. *Mini-Rev. Med. Chem.* **2011**, *11*, 185; (b) Reyland, M. *Front. Biosci.* **2009**, *14*, 2386; (c) Steinberg, S. *Physiol. Rev.* **2008**, *88*, 1341.
5. (a) Hampson, P.; Kavanagh, D.; Smith, E.; Wang, K.; Lord, J. M.; Ed Rainger, G. *Cancer Immunol. Immunother.* **2008**, *57*, 1241; (b) Ersvaer, E.; Kittang, A. O.; Hampson, P.; Sand, K.; Gjertsen, B. T.; Lord, J. M.; Bruserud, Ø. *Toxins* **2010**, *2*, 174; (c) Rosen, R. H.; Gupta, A. K.; Tyring, S. K. *J. Am. Acad. Dermatol.* **2012**, *3*, 486; (d) Stahlhut, M.; Bertelsen, M.; Hoyer-Hansen, M.; Svendsen, N.; Eriksson, A. H.; Lord, J. M.; Scheel-Toellner, D.; Young, S. P.; Zibert, J. R. *J. Drugs Dermatol.* **2012**, *11*, 1181.
6. Lebwohl, M.; Shumack, S.; Gold, L. S.; Melgaard, A.; Larsson, T.; Tyring, S. K. *JAMA Dermatol.* **2013**, *149*, 666.
7. Newman, D. J.; Cragg, G. M. *J. Nat. Prod.* **2007**, *70*, 461.
8. (a) Chen, A. C.; Halliday, G. M.; Damian, D. L. *Pathology* **2013**, *45*, 331; (b) Lee, E. H.; Klassen, A. F.; Nehal, K. S.; Cano, S. J.; Waters, J.; Pusic, A. L. *J. Am. Acad. Dermatol.* **2013**, *69*, e59.

9. Liang, X.; Grue-Sørensen, G.; Månsson, K.; Vedsø, P.; Soor, A.; Stahlhut, M.; Bertelsen, M.; Engell, K. M.; Högberg, T. *Bioorg. Med. Chem. Lett.* **2013**, *23*, 5624.
10. Grue-Sørensen, G.; Liang, X.; Högberg, T.; Månsson, K.; Vedsø, P. WO 2012/083954 A1, 2012; *PCT Int. Appl.* **2012**.
11. Sorg, B.; Hecker, E. Z. *Naturforsch* **1982**, *37b*, 748.
12. Liang, X.; Grue-Sørensen, G.; Petersen, A. K.; Högberg, T. *Synlett* **2012**, 2647.
13. Grue-Sørensen, G.; Liang, X.; Högberg, T. WO 2012/085189 A1, 2012; *PCT Int. Appl.* **2012**.
14. (a) Tauber, A. *Blood* **1987**, *69*, 711; (b) Lambeth, J. D. *J. Bioenerg. Biomembr.* **1988**, *20*, 709.
15. Bundgaard, H.; Hansen, J. *Int. J. Pharm.* **1981**, *3*, 197.
16. Brown, H. C.; McDaniel, D. H.; Hafliger, O. *Determ. Org. Struct. Phys. Methods* **1955**, 567–662. http://research.chem.psu.edu/brpgroup/pKa_compilation.pdf.
17. Pak, Y.; Enyedy, I. J.; Varady, J.; Kung, J. W.; Lorenzo, P. S.; Blumberg, P. M.; Wang, S. *J. Med. Chem.* **2001**, *44*, 1690.
18. (a) Blumberg, P. M.; Kedei, N.; Lewin, N. E.; Yang, D.; Czifra, G.; Pu, Y.; Peach, M. L.; Marquez, V. E. *Curr. Drug Targets* **2008**, *9*, 641; (b) Gennäs, G. B.; Talman, V.; Yli-Kauhaluoma, J.; Tuominin, R. K.; Ekokoski, E. *Curr. Top. Med. Chem.* **2011**, *11*, 1370.
19. The molecular dynamics (MD) calculations of PKCδ bound to compounds **10** and **9** were performed with MacroModel (OPLS-2005, water, TNCG minimization, 25 ps equilibrium followed by 2 ns simulation, 1.5 fs time step). The ligand and all atoms in residues within 5 Å of the ligand were allowed to move freely, while residues in a second shell of 5 Å were constrained (force constant 200) and the remaining atoms frozen. The docked pose (Fig. 2a) was used as the starting conformation for **10**. The starting conformation of the benzylether **9** was obtained by reducing the ester carbonyl to a methylene group. 500 structures were sampled for each simulation.
20. The docking of ingenol-3-benzoate **10** to the 1PTR crystal structure of the PKCδ C1 domain was performed in two steps. First, low-energy conformations (less than 21 kJ/mol) were obtained from a MacroModel conformational search (OPLS-2005, Water, TNCG minimization, Mixed torsional/Low-mode sampling, 1000 conformations). Secondly, the resulting conformations were docked rigidly with Glide XP to PKCδ with no scaling of the protein atoms. Default Glide settings were used for the ligand scaling and maximum 5 poses per conformation were kept. The highest scoring docked pose is shown in Fig. 2a, the MacroModel conformational energy of the ligand is 6.7 kJ/mol.
21. Glide and MacroModel Were Used as Implemented in the 2012-2 Software Suite; Schrödinger, LLC: New York, NY, 2012.
22. Nicholls, A. W.; Akira, K.; Lindon, J. C.; Farrant, R. D.; Wilson, I. D.; Harding, J.; Killick, D. A.; Nicholson, J. K. *Chem. Res. Toxicol.* **1996**, *9*, 1414.
23. Mainieri, F.; Paganini, A.; Ech-Chahad, A.; Appendino, G. *Nat. Prod. Commun.* **2007**, *2*, 375.
24. The quantum mechanical optimisations were performed with Jaguar. DFT was used with default settings (B3LYP, 6–31**). Solvent was set to Water (PBF model). Jaguar was used as implemented in the 2012–2 software Suite (Schrödinger, LLC, New York, NY, 2012).
25. DMSO stock solution containing a known amount of compound was diluted with pre-heated (37 °C) aqueous buffer pH 7.4 to an organic content ⩽30% v/v. After thorough shaking, the solution was placed in the HPLC auto sampler (37°C) and injected within 5 min and then repeatedly injected over a period of 16 hours. Based on the decrease of area of the compound signal (UV detection at normally 270 nm) the recovery of the compound over time was assessed.
26. Polymorphonuclear leukocytes (PMN) were isolated and purified from fresh buffy coats and incubated for 40 min at ambient temperature with titrated test compound (highest test concentration 10 μM) pre-mixed with hydroethidine. The PMN respiratory burst was quantified by measuring fluorescence expressed in relative light units at 579 nm (excitation: 485 nm) using an Envision plate reader. EC50 was calculated as the concentration of test compound producing 50% of the maximum effect given by ingenol 3-angelate (**1**). $E_{max}$ indicates the maximal response in relation to **1**.
27. Human adult log-phase primary primary epidermal keratinocytes were sub-cultured in 96-well plates at 10,000 cells/well and incubated with titrated test compound for 6 h at 37 °C in humidified air/$CO_2$ (95%/5%). Secreted TNFα levels were quantified using Meso Scale Discovery 4-spot cytokine plates. Secreted IL8 levels were quantified using Meso Scale Discovery 4-spot cytokine plates, or based on homogeneous time-resolved fluorescence (Human IL-8 HTRF® kit, CisBio). EC50 and $E_{max}$ were calculated as described in Ref. 26.
28. HeLa cells were treated with increasing concentrations of ingenol esters up to 400 μM for 30 min at 37°C. Subsequently, metabolic activity was quantified by the use of the resazurin-based dye formulation PrestoBlue (Invitrogen). $LC_{50}$ was calculated as the concentration of test compound producing 50% loss of metabolic activity.
29. PKCδ was tested in the KinaseProfiler™ assay (Millipore) using 0.05 mg/mL phosphatidylserine in the absence of diacylglycerol to allow for observations of any stimulatory effects. The compounds were serially diluted, at semilogarithmic intervals, for twelve points starting from 10 μM. Assays were started by the addition of ATP and run for 40 min at room temperature. Data points for the $EC_{50}$ determinations were performed in duplicate.